

**SEISMIC RESPONSE OF A NINE-STORY STEEL FRAME
WITH FRICTION DAMPED CROSS-BRACING**

Ian D. Aiken¹, James M. Kelly², and Avtar S. Pall³

¹ Graduate Student, Dept. of Civil Engineering, University of California, Berkeley, USA

² Professor, Dept. of Civil Engineering, University of California, Berkeley, USA

³ President, Pall Dynamics Limited, Montreal, Quebec, Canada

SUMMARY

A passive energy dissipation system that incorporates friction damping devices in the cross-bracing of a medium-rise steel moment resisting frame is investigated. Earthquake simulator tests and an analytical study of the system are performed and the response characteristics compared with those of equivalent moment resisting and eccentric braced frames.

An existing scale model 9 story steel moment resisting frame (MRF) was modified to include friction damped bracing as part of the lateral load resisting system. The frame is one bay wide and three bays long and represents a typical section in the weak direction of a steel frame building of approximately one quarter scale.

It was observed that the friction damped braced frame (FDBF) system had the ability to behave in a nonlinear fashion without demanding inelastic behavior in the frame itself. This implied continued integrity of the structure during and after a seismic event. Analytical results and experimental observations confirmed that for small variations of the slip loads from the optimum loads the overall response of the frame remained essentially unchanged.

INTRODUCTION

It is generally accepted that the performance of a structure subject to earthquake attack is enhanced by an increase in internal damping in that structure. The damping absorbs kinetic energy induced in the structure and prevents the build-up of resonant vibrations should the natural frequency of the structure coincide with a strong frequency present in the ground motion. In conventional structural design for earthquake resistance the damping in the structure is produced by inelastic action at beam-column connections and to develop significant damping the amount of inelastic action can produce damage at the connections. For long duration earthquake attack, such as, for example, the recent Mexico City earthquake, this damage at the connections over many cycles can lead to collapse of the structure even for a relatively low peak ground acceleration.

There have been attempts in recent years to introduce special structural details such as the eccentrically braced frame, or special energy absorbing devices which can increase the damping of the system but still sustain many cycles of action without leading to collapse. The action in the eccentric braced frame and in many of the devices so far proposed is still cyclic plastic deformation and as such is irrevocably associated with the development of local damage. While the devices could in principle be replaced after a severe earthquake, eccentric bracing is an integral part of the structure and could not be replaced. Further, in both cases the response of the element and of the entire structural system can be complex and there are as yet unresolved problems in designing structures using design spectrum methods (which are the most widely used techniques and which are intrinsically linear).

The use of frictional damping elements for a variety of structural systems has been proposed by Pall, ranging from braced frames [1,2] to concrete shear walls [3] and panel structures [4]. Frictional elements have the advantage of being amenable to a particularly simple form of mechanical modelling and their response should be repeatable and fatigue resistant. The system which is the subject of this experimental study also has the added advantage that it can be incorporated directly in the bracing of a structural frame. The energy dissipated by a typical friction damping device is proportional to the slip load and the slip deformations of that device. For some specific slip load, or combination of device slip loads within a structure, an optimum (minimum) response for the FDBF can be achieved.

TEST PROGRAM

Experimental Model

The earthquake simulator tests were performed on a nine story 1/4-scale steel frame structure which was 28ft high and 18ft wide. To satisfy similitude requirements the structure was loaded with additional mass, consisting of 10 kips of concrete and lead ballast per level, giving a total structure weight of approximately 99 kips. The scale model was originally constructed for an experimental investigation into the effects of column uplift on the seismic performance of structures [5] and has also been used in a previous series of base isolation tests [6]. The structure was modified for the friction damping tests by providing suitable connection details at the interior beam-column joints to allow the installation of the friction devices. The structure with the friction damping devices installed in the bracing is shown in Figure 1.

Friction Damping Devices

The friction damping devices used in the test series were of a design originally proposed by Pall. A typical friction damping device is shown in Figure 2, and consists of diagonal brace elements that have a friction interface at their intersection point and which are connected together by horizontal and vertical link elements. The friction interface is a simple brake-pad lining/stainless steel couple which is activated by a specified preload normal force. The link elements ensure that when the load applied to the device via the braces is sufficient to initiate slip of the tension arm then the compression arm will also slip

an equal amount in the opposite direction. Deformation fields of a friction damping device are shown in Figure 3. Implicit with these slip deformations, and hence energy dissipation by the devices, is that the structural frame must undergo geometric deformations. The design intent, therefore, is to select the loads required to cause slip in the devices within the frame to correspond to the range of elastic deformations of the structure. The criteria used to determine the slip loads for the devices are outlined below:

? The damping devices should not slip for wind and low to moderate earthquake loadings or shear forces calculated on the basis of a quasi-static approach as typically specified by the building codes. This requirement leads to a minimum value for the slip load.

? The devices should start slipping before the yield limit of any member of the structure is reached. This places an upper bound on the device slip load.

? The slip loads of the devices should be such that the energy dissipated within the structural system due to friction is maximized.

These criteria were used to obtain an approximate value for the slip loads required in the devices, and then the optimization of the loads was achieved by performing a series of nonlinear time history analyses, varying the slip loads and evaluating response amplitudes. It has been observed previously by Filiatrault and Cherry [7] that variations of +/- 20% in the optimum slip load do not significantly alter the overall response of a friction damped structure; and with the above criteria as a basis for selection, slip loads as shown in Figure 4 were chosen. The slip load in a device is obtained by varying the applied preload normal force, and for experimental purposes, preliminary tests of a single device in a static test rig were performed to calibrate device slip load (P_s) against preload normal force (which was measured in terms of the torque applied to the center bolt}. Hence, specified slip loads could be easily obtained or changed within the model structure as necessary during testing.

Preliminary Tests of Model

Following the modifications to the frame and the installation of the friction damping devices, preliminary tests were conducted to determine the dynamic characteristics of the model structure. These initial tests consisted of white noise base motion and an impulse excitation, and from the data collected modal frequencies and an estimate of the initial damping of the structure were calculated.

The white noise input motion had an almost constant Fourier amplitude for the frequency range of 0 to 10 Hz. By taking transfer functions of the roof acceleration time history the modal frequencies were estimated. The fundamental frequency of the FDBF was estimated to be 2.23 Hz and the second mode frequency to be 8.34 Hz. The same method was used for the frame in the MRF configuration and the first two frequencies were found to be $f_1 = 2.00$ Hz and $f_2 = 6.61$ Hz.

The impulse loading consisted of a square wave input to the shaking table and was used to excite free vibration responses in the model. These tests were used to obtain an estimate of the damping of the structural system. By evaluating the logarithmic free vibration decay of the 9th floor displacement signal damping in the FDBF was found to be $\epsilon = 5.6\%$ and $\epsilon = 2.4\%$ for the MRF. The damping in the FDBF was dependent on the level of excitation and the amount of slip in the friction devices and so the value of 5.6% was only applicable for low levels of excitation during which there was essentially no slip in the devices. As soon as the level of excitation was such that the devices began to slip the amount of damping in the structural system increased significantly.

Earthquake Tests of Model

Earthquake testing of the model was conducted using 10 different real and synthesized earthquake signals that provided a wide range of characteristics of earthquake motion. The earthquake signals used for testing were El Centro, 1940; Kern County Taft, 1952; San Francisco, 1957; Parkfield, 1966; Pacoima Dam, 1971; Bucharest, 1977; Miyagi-Ken-Oki (MKO), 1978; Mexico City, 1985 and two synthesized signals with response spectra equivalent to the ATC 3-06 spectrum for soil type 1. A range of magnitudes of excitation were used for the El Centro, Mexico City, Taft and Miyagi-Ken-Oki earthquakes to gain an insight to the change in response of the structure with varying level of disturbing force.

Tests using the Mexico City signal were also performed using modified time-scale factors. Similitude laws require that for the 1/4-scale model the earthquake signals be time scaled by a factor of $1/(\text{scale factor}^{0.5}) = 1/2$. However, a modified time scale factor was arbitrarily imposed on the Mexico City signal to move the predominant frequency of the signal to coincide with (or be very close to the first frequency of the FDBF structure. This resulted in a quasi-resonance excitation and very large responses were obtained in the structure. This technique was used for tests of both the FDBF and the MRF, and the effects on response due to the friction devices were able to be evaluated.

For the remaining earthquake signals, the tests performed were moderate level excitations, and these were intended for comparisons with previous tests conducted on the model as an eccentrically braced frame (EBF) and in the MRF configuration.

TEST RESULTS

Hysteresis Loops And Damping

For any frictional system the amount of energy dissipated by the system and the damping in the system are proportional to the slip excursions of the frictional elements. This means that frictional damping elements in a structural system will become relatively more effective as the magnitude of the input force increases. This pattern was observed in the series of tests using the El Centro, Taft, Mexico City and Myagi-

Ken-Okii signals for a range of increasing input accelerations. The gradual decrease in the transmissibility (roof acceleration/table acceleration) with increasing peak table acceleration (PGA) can be seen from the data in Table 1.

As a result, values for damping calculated from hysteresis loops for the devices increased as PGA increased. A typical hysteresis loop for a device at the bottom level of the structure is shown in Figure 5. This loop is plotted for the Miyagi-Ken-Okii PGA = 0.447g test. The total force in the device is the sum of the forces in the tension and the compression braces, and this is plotted against the slip deformation time history of the device to obtain a hysteresis loop. The equivalent viscous damping ratio for this loop is $e=37.6\%$, and the effective stiffness of the device at this level of excitation is $k_{eff} = 31.8$ kips/inch. Similar loops for the same device for the El Centro PGA = 0.170g test yielded values of $e = 22.4\%$ and $k_{eff} = 47.2$ kips/inch, and for the El Centro PGA = 0.838g test, $e = 32.2\%$ and $k_{eff} = 29.9$ kips/inch. Clearly, there is a significant increase in damping and decrease in device effective stiffness with the increase in magnitude of the input motion. For other earthquakes, damping provided by individual friction devices was observed to be in the range of 8.5% - 37.6%.

To obtain an estimate of the total damping in the FDBF, hysteresis loops of base shear plotted against first floor relative displacement were evaluated for equivalent viscous damping. Such a hysteresis loop is shown in Figure 6 for the Miyagi-Ken-Okii PGA @ 0.447g test. The damping ratio for this test is $= 16.7\%$. During the preliminary tests damping of about $e = 2.4\%$ was calculated for the MRF. Thus, the addition of the frictional elements has added approximately a further 14% to the damping in the structure. This is a significant increase in damping in a structure. For other large magnitude tests damping in the range of 15% to 16.7% was observed, and for smaller magnitude tests typical values of damping were 7% to 10%.

Energy Dissipation

A clear indication of the effectiveness of the friction damping devices in the structural system is given by a consideration of energy dissipation in the structure. Two approaches were taken for the evaluation of the amount of energy dissipated. These were: (a) calculating the amount of the total energy in the structure at a particular level by integrating the inertial story shear force (the sum of all the inertial story forces above the level in question) with respect to the story drift time history and comparing this value with the amount of energy dissipated by the friction devices at that level, and (b) determining the total energy input to the structure by integrating the base shear force with respect to the shaking table displacement and comparing this energy with the total energy dissipated by all the devices in the structure.

A typical energy time history for a level 1 device obtained using the first approach is given in Figure 7. At the completion of the earthquake the device has absorbed 93% of the energy input to that level. For devices at other levels and other earthquake inputs this value varied

between about 93% for the bottom level to about 60 - 70% for the upper levels of the structure. To obtain the total energy dissipated by the devices during an earthquake the known values were interpolated to give approximate values of dissipation at the other levels. Time histories of total input energy and approximate energy dissipated by all devices during the Mexico City PGA = 0.651g test are shown in Figure 8. The total energy dissipated by all the friction devices is approximately 70% of the total input energy. The fact that this ratio is not higher reflects that the distribution of device slip forces in the model was not optimized for this earthquake motion.

Negligible change in structure frequency was observed (even for very large magnitude tests) due to the nonlinear slip behavior of the friction devices. Changes in frequency of the order of 1 - 2% at most were observed during testing.

Comparison to NMF Test Results

The most significant comparisons of response between the FDBF and the MRF are found for the tests performed using the modified Mexico City signal. For both structural systems the magnitude of the input signal was increased until a maximum relative displacement of 2.8 - 3.0 inches was achieved. Any displacements beyond this would have caused excessive damage to the frame, and thus were undesirable because of the need for further tests.

The maximum peak input acceleration experienced by the FDBF was PGA = 0.651g, and corresponding to this motion was a maximum relative displacement in the model of 2.80 inches. A comparable test of the MRF had a PGA @ 0.249g and for this test the model underwent a maximum relative displacement of 3.11 inches. Figure 9 shows the profile of peak story accelerations normalized to PGA for these two tests, and in Figure 10 the profiles of maximum story drift normalized to PGA are given. The ratios of MRF response/FDBF response for these two tests are 2.91 for displacement and 2.02 for acceleration.

Story Shears

For the PGA = 0.651g test the FDBF experienced a peak base shear of 69.9 kips. The story shear profile determined at the time of peak base shear is shown in Figure 11. Also shown in this figure is the profile of shear force resisted by the friction damping devices. Figure 12 gives the profile of story shears at the time of peak base shear for the IMF subjected to the PGA = 0.249g test. For this test the peak base shear was 64.2 kips, all of which was required to be resisted by damaging inelastic action of the MRF elements.

CONCLUSIONS

The seismic performance of the frame is considerably enhanced by the inclusion of the friction damping devices in the structural system. It is clear that the devices provide a significant increase in the

available damping within the structure and that this leads to a direct improvement in performance. The dissipation characteristics of the friction damping mechanisms are reliable and the devices are not damaged by large loads. The devices become more effective in absorbing energy as the magnitude of the disturbing force increases. By confining the energy dissipation to the friction devices which are specifically designed to perform under extreme loading conditions without sustaining damage, the main structural elements are able to remain elastic.

The difference between structural systems appears less dramatic from considerations of shear force, but it is still shown that a large portion of the base shear force in a structure can be resisted in a controlled manner and not be required to be resisted by inelastic action of primary structural elements.

REFERENCES

- [1] Pall, A. S., Marsh, C., "Response of Friction Damped Braced Frames", Journal of the Structural Division, American Society of Civil Engineers, Vol. 108, No. ST6, June 1982.
- [2] Pall, A. S., "Response of Friction Damped Buildings", Proceedings of the Eighth World Conference on Earthquake Engineering, San Francisco, Vol. V, 1984.
- [3] Pall, A. S., Marsh, C., "Friction Damped Concrete Shear Walls", Journal of the American Concrete Institute", No. 3, Proceedings Vol. 78, 1981.
- [4] Pall, A. S., Marsh, C., Fazio, P., "Friction Joints for Seismic Control of Large Panel Structures", Journal of the Prestressed Concrete Institute, Vol. 25, No. 6, 1980.
- [5] Arthur A. Huckelbridge, "Earthquake Simulation Tests of a Nine Story Steel Frame with Columns Allowed to Uplift", Report No. UCB/EERC-77/23, Earthquake Engineering Research Center, University of California, Berkeley, (1977).
- [6] Griffith, M. C., Aiken, I. D., Kelly, J. M., "Experimental Evaluation of Seismic Isolation of a Nine Story Braced Steel Frame Subject to Uplift", Report No. UCB/EERC-87/03.
- [7] Filiatrault, A. and Cherry, S., "Performance Evaluation of Friction Damped Steel Frames Under Simulated Earthquake Loads", Earthquake Engineering Laboratory Report, Dept. of Civil Engineering, University of British Columbia, Vancouver, B. C., Canada, 1985.

EARTHQUAKE SIGNAL	SPAN	TIME SCALE	PK. TABLE ACCEL. (g±)	PK. STRUCT. ACCEL. (g±)	AMPLIF. TABLE
El Centro	150	1/2	0.321	0.953	2.982
	225	1/2	0.422	1.219	2.899
	300	1/2	0.552	1.458	2.638
	350	1/2	0.719	1.548	2.183
	400	1/2	0.838	1.592	2.007
Tah	200	1/2	0.409	0.953	2.310
	300	1/2	0.812	1.230	2.073
	350	1/2	0.777	1.602	2.082
Shake	40	1/3	0.115	0.695	6.013
	80	1/3	0.219	1.089	4.772
	120	1/3	0.428	1.389	3.214
	160	1/3	0.687	1.519	2.207
SBCD	150	1/2	0.170	0.917	4.992
	200	1/2	0.266	1.002	4.861
	275	1/2	0.307	1.282	4.505
	350	1/2	0.417	1.208	2.920

Table 1 Reduction in Transmissibility Ratio With Increasing Peak Table Acceleration

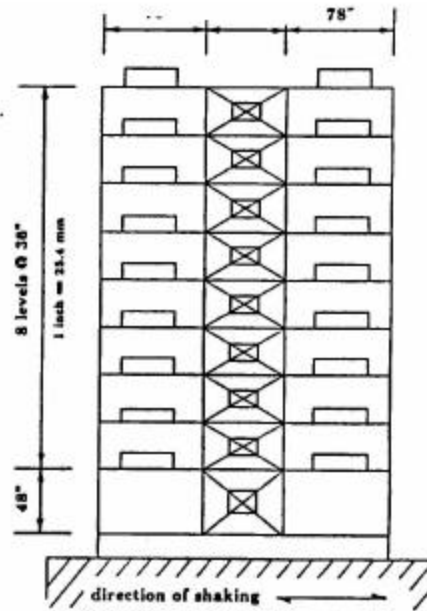


Figure 1 8-Story Steel Friction Damped Braced Frame

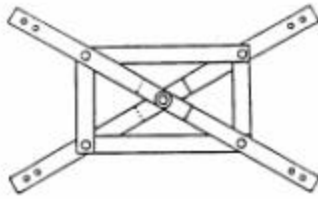


Figure 2 Friction Damping Device

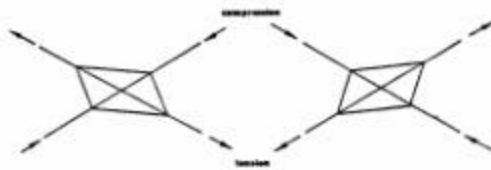


Figure 3 Deformed Configurations of a Friction Damping Device

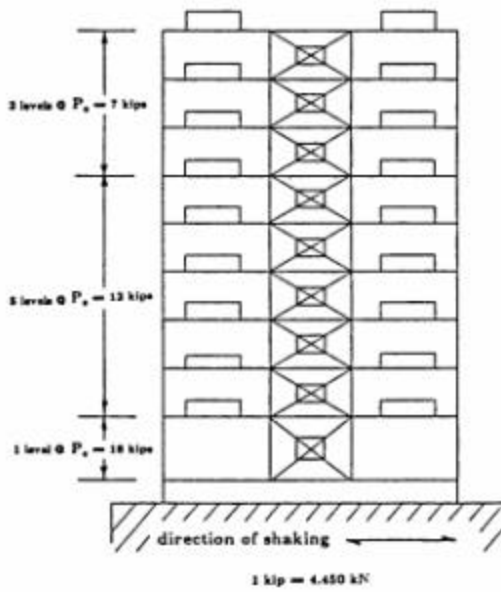


Figure 4 Distribution of Slip Forces

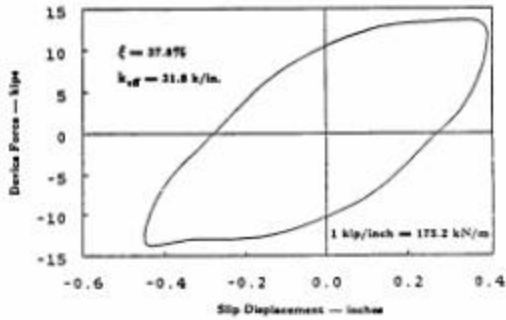
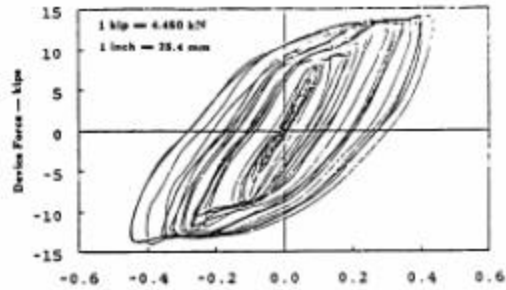


Figure 5 Device Hysteretic Loop — MKO, pgs = 0.447g

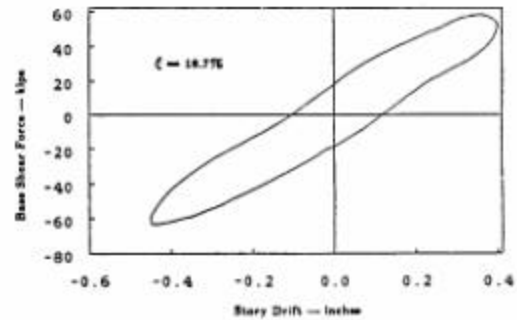
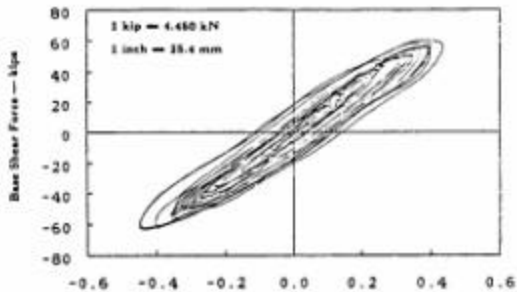


Figure 6 Base Shear vs. First Floor Drift — MKO, pgs = 0.447g

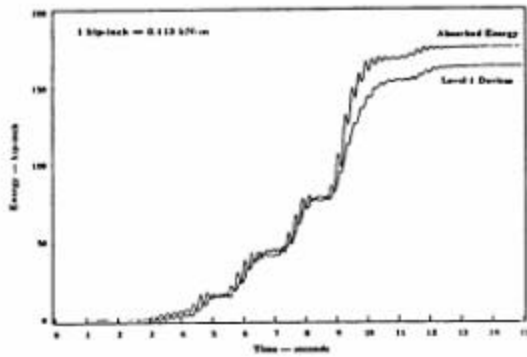


Figure 7 Level I Energy Time History -- Mexico City, $pga = 0.851g$

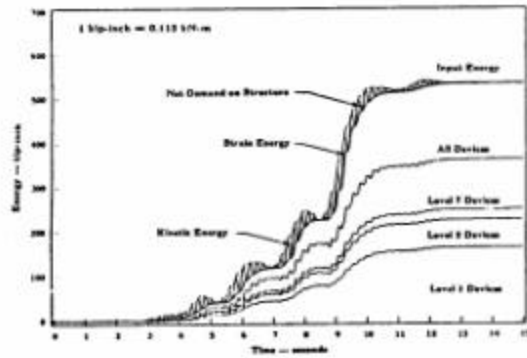


Figure 8 Total Energy Time History -- Mexico City, $pga = 0.851g$

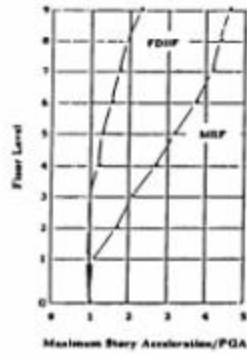


Figure 9 Peak Story Acceleration Profile

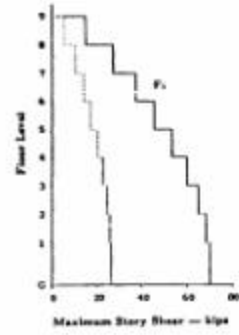


Figure 11 Story Shear Profile -- Mexico, $pga = 0.851g$

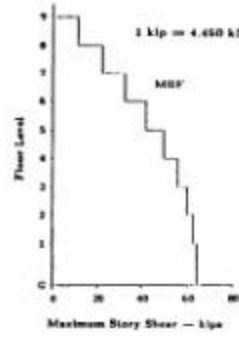


Figure 12 Story Shear Profile -- Mexico, $pga = 0.210g$

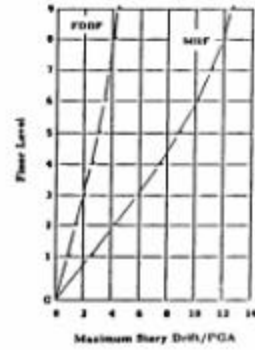


Figure 10 Peak Story Drift Profile